

VEGF-mediated disruption of endothelial CLN-5 promotes blood-brain barrier breakdown

Azeb Tadesse Argaw^a, Blake T. Gurfein^a, Yueting Zhang^a, Andleeb Zameer^a, and Gareth R. John^{a,b,1}

^aCorinne Goldsmith Dickinson Center for Multiple Sclerosis and Department of Neurology, Mount Sinai School of Medicine, New York, NY 10029; and ^bDepartment of Pathology, Albert Einstein College of Medicine, Bronx, NY 10461

Edited by Berislav Zlokovic, University of Rochester Medical Center, Rochester, NY, and accepted by the Editorial Board December 5, 2008 (received for review September 2, 2008)

Breakdown of the blood-brain barrier (BBB) is an early and significant event in CNS inflammation. Astrocyte-derived VEGF-A has been implicated in this response, but the underlying mechanisms remain unresolved. Here, we identify the endothelial transmembrane tight junction proteins claudin-5 (CLN-5) and occludin (OCLN) as targets of VEGF-A action. Down-regulation of CLN-5 and OCLN accompanied up-regulation of VEGF-A and correlated with BBB breakdown in experimental autoimmune encephalomyelitis, an animal model of CNS inflammatory disease. In cultures of brain microvascular endothelial cells, VEGF-A specifically down-regulated CLN-5 and OCLN protein and mRNA. In mouse cerebral cortex, microinjection of VEGF-A disrupted CLN-5 and OCLN and induced loss of barrier function. Importantly, functional studies revealed that expression of recombinant CLN-5 protected brain microvascular endothelial cell cultures from a VEGF-induced increase in paracellular permeability, whereas recombinant OCLN expressed under the same promoter was not protective. Previous studies have shown CLN-5 to be a key determinant of trans-endothelial resistance at the BBB. Our findings suggest that its down-regulation by VEGF-A constitutes a significant mechanism in BBB breakdown.

CNS | cytokine | inflammation | tight junction

The blood-brain barrier (BBB) acts as a selective interface separating the CNS parenchyma from the systemic circulation (1). The barrier exists at the level of brain microvessel endothelial cells (BMVECs), which use tight junctions to restrict paracellular permeability (2). Transmembrane proteins regulating tight junction organization include claudins (CLNs) and occludin (OCLN). Claudins act as the main determinants of tight junction properties (3), and BMVECs predominantly express CLN-5, with smaller amounts of CLN-3 and CLN-12 (4). Transfection studies show that CLN-5 plays a key role in the appearance of BBB properties (5), and CLN-5^{-/-} mice display selective BBB opening (6). OCLN is also a tight junction strand component, and contributes to junction properties and regulates permeability (7), but strands form normally in OCLN-deficient cells (8), and OCLN^{-/-} mice display a complex phenotype (9). Formation of the endothelial barrier is not intrinsic and depends on other lineages. Astrocytes have been implicated in the induction and maintenance of barrier properties (10), and pericytes are also known to regulate microvessel structure and permeability (11, 12).

Whereas the phenotype of the BBB is well understood, the mechanisms underlying its disruption in disease have remained elusive. Loss of BBB integrity is an early and prominent pathological feature of inflammatory CNS disorders and is also observed in neoplastic and degenerative conditions (1, 2). Disruption of the BBB leads to dysregulation of CNS interstitial fluid and edema (13), and allows entry into the parenchyma of inflammatory mediators, antibodies, and complement and plasma proteins associated with potentiation of inflammation and restriction of repair (14). As astrocytes are believed to play important roles in BBB induction and maintenance, they have also been proposed as inducers of barrier disruption (15). Recently, we investigated potential links between astrocyte reactivity and BBB breakdown. Compatible with

reports from other groups, our results implicated the transcription factor hypoxia-inducible factor-1 α and its effector VEGF-A in these events (16). VEGF-A is the most important angiogenic factor in the developing CNS (17, 18) and a potent inducer of BBB disruption in adults (19, 20). Studies including our own have localized VEGF-A to reactive astrocytes in inflammatory CNS lesions (16), but the mechanisms underlying its effects on the BBB remain unknown.

Here, we show that VEGF-A disrupts expression of both CLN-5 and OCLN in BMVEC cultures in vitro and in the CNS in vivo. Down-regulation of both proteins also accompanies up-regulation of VEGF-A and correlates with BBB opening in experimental autoimmune encephalomyelitis (EAE), a widely used animal model of CNS inflammation. Importantly, our functional studies suggest that loss of CLN-5 is a central event in determining BBB disruption, whereas the role of OCLN is less easily defined. These data implicate VEGF-mediated down-regulation of CLN-5 as a significant mechanism in BBB breakdown. These events may represent a potential target for therapeutic intervention in inflammatory CNS disease.

Results

In EAE, BBB Disruption Increases as Endothelial CLN-5 and OCLN Decrease. To investigate whether BBB breakdown in CNS inflammatory disease is associated with changes in endothelial tight junction proteins, we examined samples from mice with EAE induced in 8-week C57BL/6 animals using myelin-oligodendrocyte glycoprotein 35–55 (MOG_{35–55}) as described (21) [Fig. 1, [supporting information \(SI\) Fig. S1](#)]. An ascending flaccid paralysis (see *Materials and Methods*) was apparent from 10–12 d after induction (21), and animals were killed at 10–30 d. CNS tissue sections were immunostained for CLN-3, CLN-5, CLN-12, and OCLN, plus fibrinogen and albumin as markers of BBB disruption (19). Confocal imaging of cortex and spinal cord from age- and sex-matched controls (10–12 weeks) showed that CLN-5 and OCLN localized to linear profiles, confirmed as vessels using Factor VIII-related antigen (Fig. 1A). Staining for GFAP illustrated the close proximity of astrocytic end-feet to these vessels (Fig. 1A).

In lumbar spinal cord of animals with EAE (paraparesis/paraplegia, 15–18 d after induction), typical perivascular inflammatory lesions were observed in white matter (Fig. 1B and C), and confocal imaging demonstrated widespread BBB breakdown as assessed by parenchymal immunoreactivity for fibrinogen and albumin (Fig. 1D and F). Importantly, CLN-5 and OCLN immunoreactivity also appeared reduced in these areas (Fig. 1D and F). CLN-3 and CLN-12 were not reliably detected in EAE samples or

Author contributions: A.T.A., B.T.G., Y.Z., and A.Z. performed research; G.R.J. designed research.

The authors declare no conflict of interest.

This article is a PNAS Direct Submission. B.Z. is a guest editor invited by the Editorial Board.

¹To whom correspondence should be addressed. E-mail: gareth.john@mssm.edu

This article contains supporting information online at www.pnas.org/cgi/content/full/0808698106/DCSupplemental.

© 2009 by The National Academy of Sciences of the USA

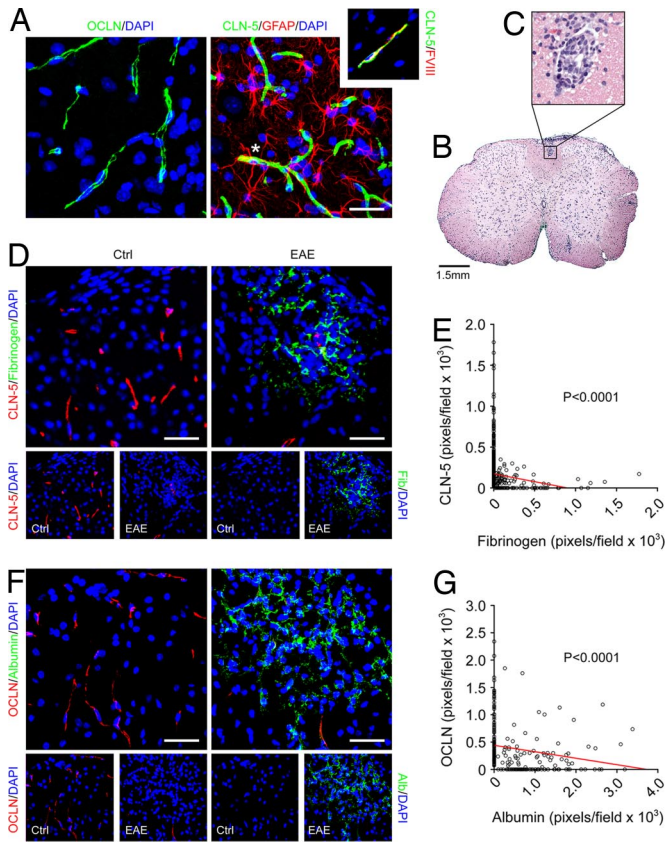


Fig. 1. In EAE, BBB disruption increases as endothelial CLN-5 and OCLN decrease. (A) Confocal Z-series projections of cerebral cortex from adult mice (C57BL/6, 11 weeks) immunostained for OCLN (Left) or CLN-5 plus GFAP (Right). CLN-5 and OCLN localize to linear profiles, confirmed as vessels using Factor VIII-related antigen (Right, Inset). Staining for GFAP illustrates close proximity of astrocytic end-feet to vessels (Right, asterisk). (B and C) Hematoxylin and eosin-stained section of lumbar spinal cord from 10-week C57BL/6 mouse 16 days after induction of EAE with MOG_{35–55}. Perivascular inflammation is observed in white matter, illustrated at higher magnification in C. (D and F) Confocal Z-series projections of dorsolateral lumbar spinal cord from 10-week C57BL/6 mice with EAE (tail paralysis and paraparesis, Right) 15–18 days after induction, or age- and sex-matched controls (Left), immunostained for CLN-5 and fibrinogen (D) or OCLN and albumin (F). EAE sections display disruption of the BBB as assessed by parenchymal immunoreactivity for fibrinogen or albumin. Immunoreactivity for CLN-5 and OCLN appears reduced in these areas. Individual channels are presented below each image for clarity. (E and G) Morphometric analysis (see Materials and Methods) confirms a significant correlation between BBB disruption and decreased immunoreactivity for CLN-5 and OCLN in EAE sections (E, $P < 0.0001$; G, $P < 0.0001$, Spearman rank correlation). Results shown are from individual animals with EAE (the same illustrated in D and F), and are representative of findings from 3 experiments with 5 animals per condition per experiment. (Scale bars: A, 50 μm ; B, 1.5 mm; D and F, 100 μm .)

controls (not shown). To quantify these findings, we used morphometric analysis of Z-series projections (Fig. 1 E and G). Pixels positive for CLN-5, OCLN, fibrinogen, and albumin were counted in projections from lumbar spinal cord in 5 animals with EAE and 5 controls (see Materials and Methods). These analyses revealed a significant correlation between the observed BBB disruption in animals with EAE and decreased CLN-5 and OCLN immunoreactivity (Fig. 1E, $P < 0.0001$; Fig. 1G, $P < 0.0001$).

To define the time course of changes in CLN-5 and OCLN in EAE, we killed animals at clinical onset (10–12 d) and during the acute clinical phase (15–18 d, as described earlier) and more chronic clinical plateau (28–30 d; Fig. S1A). Sections of lumbar spinal cord from all three time points and controls were immunostained for CLN-5 or OCLN plus fibrinogen or albumin and imaged as

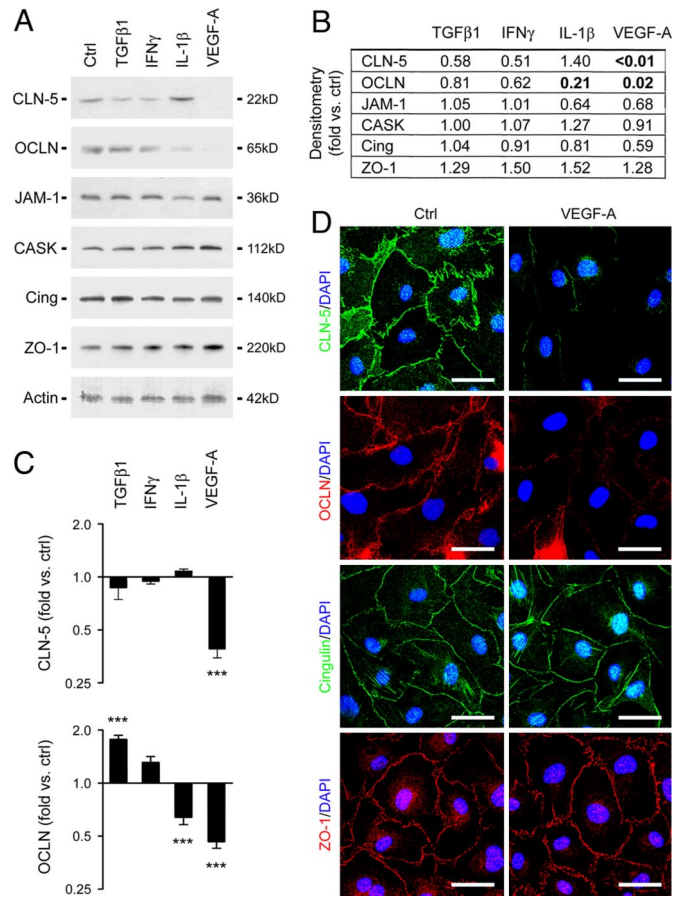


Fig. 2. VEGF down-regulates CLN-5 and OCLN in human BMVECs. (A) Immunoblots of protein extracts from human BMVEC treated for 24 h with cytokines shown (VEGF-A, 100 ng/mL; other cytokines, 10 ng/mL). (B) Results in blots quantified by densitometry (see Materials and Methods). Note that CLN-5 and OCLN are both strongly down-regulated by VEGF-A. OCLN is also down-regulated by IL-1 β . Other tight junction-associated adaptor and regulatory proteins shown include JAM-1, CASK, ZO-1, and cingulin, which are unchanged in response to inflammatory stimuli. (C) Results of real-time PCR performed on cDNA from human BMVEC treated as described earlier. Results for CLN-5 and OCLN are illustrated. Note that CLN-5 and OCLN mRNA are both strongly down-regulated by VEGF-A. OCLN mRNA is also down-regulated by IL-1 β and up-regulated by TGF β 1. *** $P < 0.001$, ANOVA followed by Bonferroni post-test. (D) Confocal imaging of human BMVEC treated with 100 ng/mL VEGF-A for 24 h and immunostained for CLN-5, OCLN, cingulin and ZO-1. In controls, all four proteins localize to the plasma membrane in areas of cell-cell contact. Note that CLN-5 and OCLN are both down-regulated by VEGF-A. (Scale bars: D, 20 μm .) Data in all panels are representative of at least 3 separate experiments on 3 distinct cultures.

described earlier (Fig. S1B and C). Consistent with previous reports (22), in mice with EAE, BBB breakdown was mild at onset of clinical signs and more widespread at 15–18 d, and persisted at 28–30 d. Importantly, BBB disruption at 28–30 d was accompanied by a persistent reduction in CLN-5 and OCLN (Fig. S1B and C). Collectively, these results demonstrate a strong correlation between BBB breakdown and decreased endothelial CLN-5 and OCLN in EAE. These changes persist to at least 28–30 d after induction.

VEGF Down-Regulates CLN-5 and OCLN in Human BMVECs. To define the mechanism underlying these events, primary human BMVEC cultures were treated with cytokines relevant to inflammatory CNS disease, including TGF β 1, IL-1 β , IFN γ , TNF α , and VEGF-A (Fig. 2). Protein and RNA were extracted at 6–48 h and analyzed by immunoblotting (Figs. 2 A and B) and real-time PCR (Fig. 2C). Parallel cultures were immunostained for confocal imaging (Fig. 2D).

Immunoblotting for CLN-3, CLN-5, CLN-12, and OCLN showed that CLN-5 and OCLN were both down-regulated by VEGF-A, an angiogenic factor implicated as an inducer of BBB disruption (16–20) (Fig. 2A). CLN-5 was detected as a band at 22 kD, and was strongly down-regulated by VEGF-A (Fig. 2a). Quantification using densitometry (see *Materials and Methods*) revealed that levels of CLN-5 protein were more than 100 times lower in VEGF-treated cultures than controls at 24 h (Fig. 2B). OCLN was visualized as a band at 65 kD and was also down-regulated strongly by VEGF-A and weakly by IL-1 β (Fig. 2A). Levels of OCLN protein were 50 times lower in VEGF-treated cultures and fivefold lower in IL-1 β -treated cultures than controls at 24 h (Fig. 2B). CLN-3 was observed as a weak band at 22 kD that did not change in response to inflammatory cytokines (not shown), whereas CLN-12 was not detected (not shown). We also analyzed the expression of other tight junction-associated proteins, including junctional adhesion molecule 1–3 (JAM1–3), the adaptors calcium-dependent serine protein kinase (CASK), zonula occludens 1 (ZO-1), and cingulin, and the regulatory molecules multi-PDZ domain protein 1 and membrane-associated guanylate kinase with inverted domain structure 1 (2). All were expressed in BMVEC and were unchanged in response to inflammatory stimuli (Fig. 2A; JAM-1, CASK, ZO-1, and cingulin illustrated).

Further immunoblotting showed that neither CLN-5 nor OCLN was responsive to VEGF-C, IL-6, or FGF-1 (not shown). In time-course studies, down-regulation of CLN-5 and OCLN was detected from 6 h following VEGF-A treatment, and both were undetectable through 48 h (not shown). Real-time PCR confirmed down-regulation of CLN-5 and OCLN mRNA by VEGF-A (Fig. 2C). OCLN mRNA was also down-regulated by IL-1 β and up-regulated by TGF β 1 (Fig. 2C). These studies also confirmed the expression profiles of other junction proteins analyzed in immunoblotting experiments (not shown).

Confocal imaging of immunostained cultures confirmed that, in human BMVEC cultures, CLN-5 and OCLN and associated proteins including ZO-1 and cingulin localized to plasma membrane in areas of cell-cell contact (Fig. 2D). CLN-5 and OCLN expression were disrupted by VEGF-A (Fig. 2D). Collectively, these results identify VEGF-A as a factor that down-regulates CLN-5 and OCLN in human BMVECs.

Up-Regulation of VEGF-A Accompanies Down-Regulation of CLN-5 and OCLN in the Inflamed CNS. To determine whether the effects of VEGF-A on CLN-5 and OCLN in BMVEC cultures in vitro reflected the inflamed CNS in vivo, lumbar spinal cord sections from animals with EAE (paraparesis/paraplegia, 15–18 d after induction) and controls were immunostained for VEGF-A plus CLN-5, OCLN, or lineage markers, and imaged by confocal microscopy (Fig. 3 and Fig. S2). In spinal cord sections from mice with EAE, VEGF-A was strongly expressed in white matter by GFAP⁺ reactive astrocytes, and was not detected in controls (Fig. 3A). Importantly, in samples from mice with EAE, double-staining of lumbar spinal cord sections for VEGF-A and CLN-5 or OCLN showed that up-regulation of VEGF-A accompanied reduced CLN-5 and OCLN immunoreactivity (Fig. S2A and C). To quantify these findings, we used morphometric analysis of Z-series projections (Fig. S2B and D). Pixels positive for CLN-5 and OCLN were counted in projections as in Fig. 1. VEGF⁺ cells were counted in the same fields and expressed as percentage of total cells (DAPI⁺). In samples from animals with EAE, the number of VEGF⁺ cells was significantly increased (Fig. S2B, $P < 0.01$; Fig. S2D, $P < 0.001$), and CLN-5 and OCLN immunoreactivity in the same fields were significantly reduced (Fig. S2B, $P < 0.01$; Fig. S2D, $P < 0.01$). These results show induction of VEGF-A in reactive astrocytes in the inflamed CNS, and confirm that its up-regulation accompanies down-regulation of CLN-5 and OCLN.

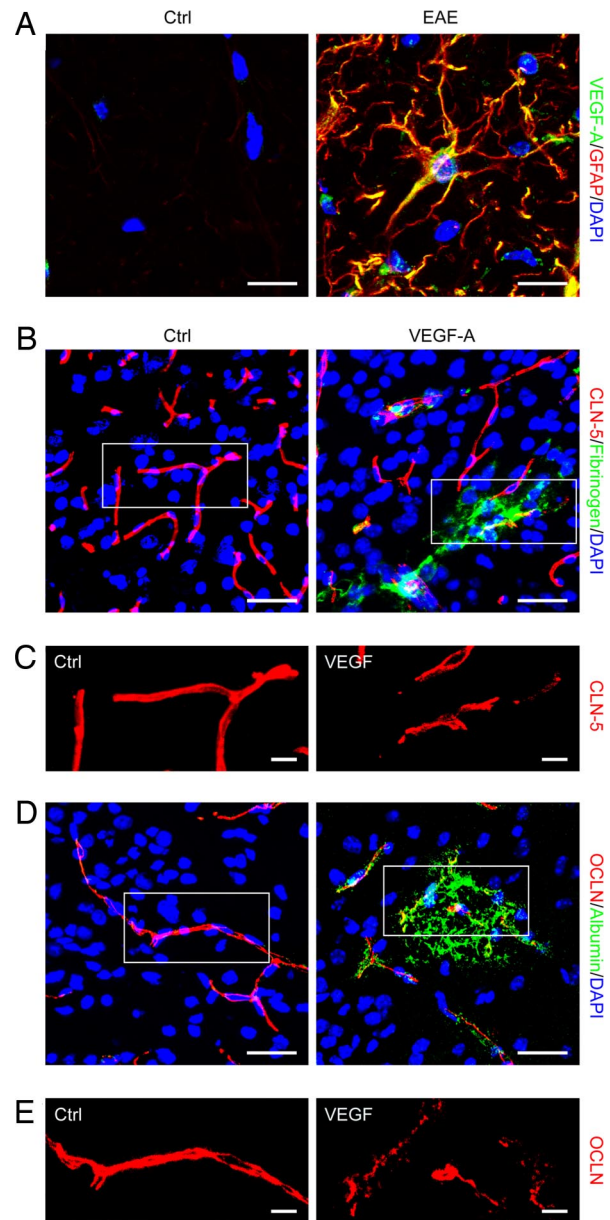


Fig. 3. VEGF-A disrupts endothelial CLN-5 and OCLN, and induces BBB permeability. (A) Confocal Z-series projection of dorsolateral lumbar spinal cord from 10-week C57BL/6 mice with EAE (as described earlier) at 16 d after induction (Right), and age- and sex-matched controls (Left), immunostained for VEGF-A and GFAP. VEGF-A immunoreactivity localizes to reactive GFAP⁺ astrocytes in the EAE sample, and is not detected in normal control. (B–E) Sections of cerebral cortex from 12-week adult C57BL/6 mice 24 h following stereotactic microinjection of murine VEGF₁₆₅ (60 ng in 3 μ L PBS/BSA, Right) or vehicle control (Left). Sections are immunostained for CLN-5 and OCLN (red channel), plus fibrinogen or albumin (green channel). The red channel from outlined areas in B and D is shown at higher magnification in C and E. Note that BBB permeability is observed around vessels in VEGF-injected areas (B and D, Right), and that immunoreactivity for CLN-5 and OCLN appears patchy and discontinuous in these areas (C and E, Right). (Scale bars: A, 20 μ m; B and D, 75 μ m; C and E, 20 μ m.) Data shown are representative of findings from at least 4 mice per time point per condition.

VEGF-A Disrupts Endothelial CLN-5 and OCLN in Vivo, and Induces BBB Breakdown. To establish whether VEGF-A regulates CLN-5 and OCLN in vivo, mouse VEGF-A (3 μ L, 20 ng/ μ L) or vehicle control was delivered into the left cerebral hemisphere of C57BL/6 mice (12 weeks), then the animals were killed at 24 h to 7 d after injection (Fig. 3 B–E). Sections of cerebral cortex were immunostained for

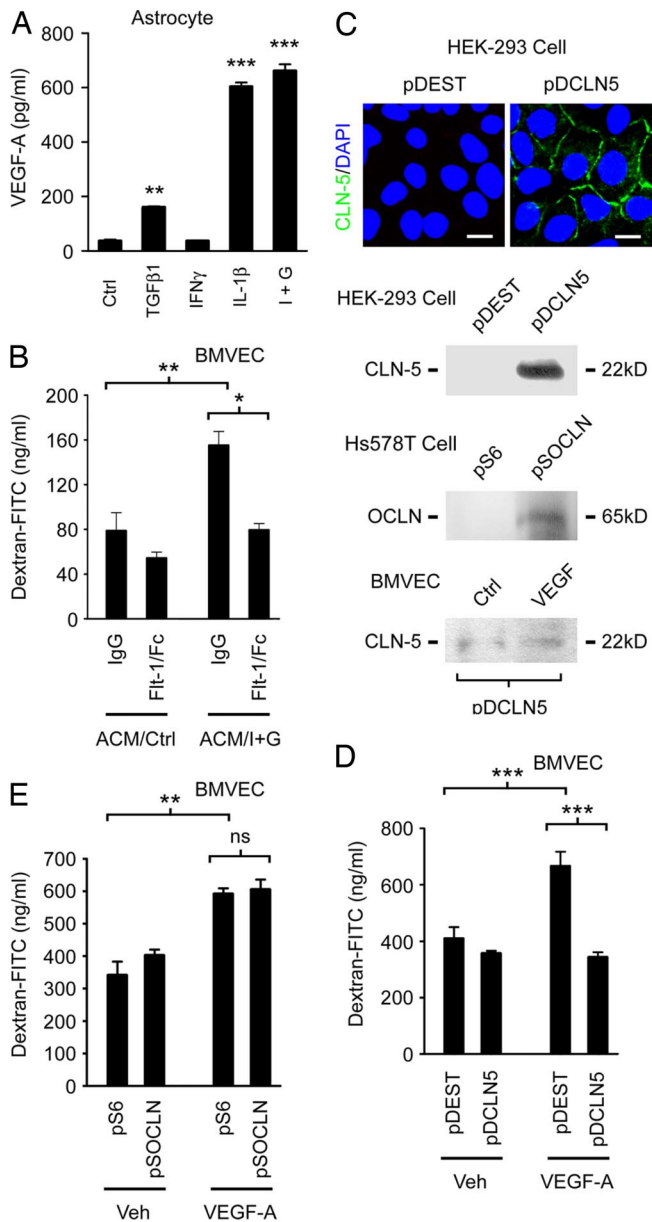


Fig. 4. VEGF-induced down-regulation of CLN-5 is a significant determinant of increased paracellular permeability in BMVEC. (A and B) Sandwich ELISA data showing secretion of VEGF-A by human astrocytes. (A) VEGF-A concentrations in astrocyte media after 24 h treatment with cytokines shown, followed by washout and culture for an additional 24 h. IL-1β is a potent inducer of VEGF-A in these cells, and its effect is potentiated by IFNγ (I+G). *** $P < 0.001$, ** $P < 0.01$, ANOVA plus Bonferroni post-test. (B) Conditioned media generated in a from IL-1β/IFNγ-treated astrocyte cultures (I+G) and controls were diluted 1:1 with CSC medium, then applied for 16 h to confluent human BMVEC monolayers on 0.4-μm culture inserts. BMVECs exposed to conditioned medium from IL-1β/IFNγ-treated astrocytes (ACM/I+G) show a significant increase in paracellular permeability, as assessed using trans-endothelial passage of 40-kD dextran-FITC. Co-treatment with 40 ng/mL Flt-1-Fc fusion protein significantly inhibits this increase in permeability (** $P < 0.01$, * $P < 0.05$, ANOVA plus Bonferroni post-test, data from 60 min following addition of 40 kD dextran). (C) Recombinant CLN-5 (pDCLN5) or OCLN (pSOCLN) or empty vector controls were nucleofected into otherwise negative cell lines (CLN-5, HEK cells; OCLN, Hs578T cells). Note expression of recombinant CLN-5 and OCLN in negative cell lines nucleofected with relevant expression construct, and localization to sites of cell-cell contact (Upper). Note also that expression of recombinant CLN-5 is refractory to 100 ng/mL VEGF-A treatment in BMVEC nucleofected with pDCLN5 (Bottom). (D and E) Bovine BMVECs were nucleofected with pDCLN5 (D) or pSOCLN (E) or empty vector controls (pDEST, pS6), then left to grow to confluence for 10–14 d on 0.4-μm inserts. Confluent monolayers were then treated with 100 ng/mL VEGF-A or vehicle control for 24 h.

CLN-5 and OCLN plus fibrinogen or albumin, then visualized by confocal imaging. Introduction of VEGF-A into adult cerebral cortex was associated with BBB opening (Fig. 3 B and D), and disruption of CLN-5 and OCLN (Fig. 3 C and E). At 24 h and 48 h, BBB breakdown was observed around vessels in VEGF-injected areas, occasionally extending deeper into the CNS parenchyma (Fig. 3 B and D, 24 h after injection illustrated). Importantly, immunoreactivity for CLN-5 and OCLN in these areas appeared patchy and discontinuous (Fig. 3 C and E). In contrast, minimal BBB disruption was observed following injection of vehicle control (Fig. 3 B and D), and CLN-5 and OCLN staining appeared smooth and continuous in vehicle-injected areas (Fig. 3 C and E). Interestingly, by 7 d after injection, CLN-5 and OCLN staining appeared normal in VEGF-injected cortex and no opening of the BBB was detectable (not shown). These findings demonstrate that VEGF-A disrupts endothelial CLN-5 and OCLN and induces BBB breakdown in the adult CNS.

Astrocyte-Conditioned Medium Induces Increased BMVEC Permeability in Vitro via VEGF-A. Collectively, these data suggested that VEGF-induced down-regulation of endothelial CLN-5 and/or OCLN may constitute a significant mechanism in BBB disruption. To test this hypothesis, we used a model system in which BMVEC are plated onto 0.4-μm pore inserts and left to mature for 10–14 d (Fig. 4). Changes in paracellular permeability are then monitored using measurements of trans-endothelial passage of dextran-FITC (40 kD and 3 kD in our studies) (23).

To establish whether astrocyte-derived VEGF-A induces increased paracellular permeability in BMVEC cultures, we exposed human BMVEC monolayers to conditioned medium from human astrocytes stimulated for VEGF-A production (Fig. 4 A and B). In preliminary ELISA studies, astrocytes were treated with IL-1β, IFNγ, or TGFβ1 for 24 h, then cytokines were washed out and replaced with fresh medium for a further 24 h. These experiments showed that IL-1β treatment was a potent inducer of VEGF-A in human astrocytes, with its effect enhanced by co-treatment with IFNγ (Fig. 4 A). In contrast, VEGF-A was not detectable in medium from human BMVEC cultures, nor induced in BMVECs in response to the same cytokines (not shown). Conditioned media from astrocytes treated with IL-1β and IFNγ and untreated controls were then diluted 1:1 with CSC medium and applied to confluent human BMVEC on inserts for 4–16 h. BMVECs exposed to conditioned medium from IL-1β/IFNγ-treated astrocytes showed a significant increase in trans-endothelial passage of dextran-FITC (Fig. 4 B, $P < 0.01$, 60 min after addition of 40 kD dextran-FITC). This was not associated with increased apoptosis on TUNEL (not shown). To define the contribution of VEGF-A, the experiment was repeated in the presence of Flt-1-Fc, a recombinant inhibitor of VEGF-A (24). Co-treatment with 40 ng/mL Flt-1-Fc significantly inhibited the observed increase in BMVEC permeability (Fig. 4 B, $P < 0.05$). These studies show that cytokine-treated human astrocytes induce an increase in paracellular permeability in BMVEC cultures, and that VEGF-A contributes significantly to this effect.

VEGF-Induced Down-Regulation of CLN-5 Is an Important Determinant of Increased Paracellular Permeability in BMVEC Cultures. To determine the relative contributions of loss of CLN-5 and/or OCLN to VEGF-A-induced BMVEC permeability, we used nucleofection to

Note that VEGF-A induces a significant increase in permeability in BMVEC monolayers nucleofected with empty vector, and that this effect is rescued in pDCLN5-nucleofected cultures (D). In contrast, the effect of OCLN expressed under the same promoter is not significant (E). *** $P < 0.001$, ** $P < 0.01$, ANOVA plus Bonferroni post-test, data shown in both panels from 60 min following addition of 40 kD dextran-FITC. (Scale bar: C, 12 μm.) Data in all panels representative of at least 5 separate experiments on 5 distinct cultures.

rescue their expression in bovine BMVECs (Figs. 4 C–E). In pilot studies, nucleofection of expression constructs into negative cell lines (CLN-5, HEK cells; OCLN, Hs578T cells) (25) resulted in expression of recombinant CLN-5 and OCLN and localization to sites of cell-cell contact (Fig. 4C). They also confirmed lack of sensitivity of the promoter used (CMV) to VEGF-A (Fig. 4C), and expression for >10 d following nucleofection (not shown). BMVECs were then nucleofected with constructs or empty vector controls, left to reach confluence on 0.4- μ m inserts for 10–14 d, then treated with 100 ng/mL VEGF-A or vehicle for 24 h, and paracellular permeability was measured (Fig. 4 D and E). These experiments identified down-regulation of CLN-5 as an important determinant of increased paracellular permeability in VEGF-treated BMVEC monolayers. In control cultures nucleofected with empty vector, as expected, VEGF-A treatment induced a significant increase in transcellular passage of dextran-FITC (Fig. 4D, $P < 0.001$, 60 min following addition of 40 kD dextran-FITC). Importantly, expression of recombinant CLN-5 strongly protected BMVEC cultures from this effect (Fig. 4D, $P < 0.001$). Similar results were obtained using 3 kD in place of 40 kD dextran (not shown). In contrast, recombinant OCLN expressed under the same promoter (CMV) did not provide significant protection (Fig. 4E, data from 60 min following addition of 40 kD dextran). Collectively, these findings implicate VEGF-induced down-regulation of CLN-5 as a significant mechanism underlying BBB disruption in the adult CNS.

Discussion

In this study, we have investigated the mechanism underlying the BBB disruption that is an early and prominent feature of CNS inflammation. Whereas the phenotype of the BBB is well understood, the mechanisms underlying its disruption in disease have remained elusive. Astrocyte-derived VEGF-A has been implicated in the response, and here we demonstrate that targets of VEGF-A action are the endothelial tight junction transmembrane proteins CLN-5 and OCLN. Importantly, our data further suggest that down-regulation of CLN-5 is central to disruption of the BBB, whereas the role of OCLN is more difficult to define. In EAE, we found that down-regulation of endothelial CLN-5 and OCLN accompanied up-regulation of VEGF-A and correlated with BBB disruption (Fig. 1 and Figs. S1 and S2). Analysis of BMVEC cultures showed that CLN-5 and OCLN protein and mRNA were selectively down-regulated by VEGF-A (Fig. 2). In mouse cerebral cortex, microinjection of VEGF-A disrupted CLN-5 and OCLN and induced barrier breakdown (Fig. 3). Functional studies revealed that expression of CLN-5 under a VEGF-insensitive promoter protected BMVEC cultures from a VEGF-induced increase in paracellular permeability, whereas OCLN expressed under the same promoter was not protective (Fig. 4). Collectively, our results implicate VEGF-mediated disruption of endothelial CLN-5 as a significant mechanism in BBB breakdown in the inflamed CNS (Fig. S3). These findings may also be relevant to neoplastic and degenerative disorders that feature BBB opening.

VEGF-A is the most potent angiogenic factor known, such that loss of a single allele results in embryonic lethality as a result of vascular abnormalities (17, 18). Its signal-transducing receptor Flk-1/VEGFR2 is expressed by BMVECs (16), and homozygous Flk-1/VEGFR2^{-/-} mice exhibit a similar phenotype to that of VEGF-A mutants and die in utero (26). Mice homozygous for loss of the non-signal-transducing receptor Flt-1/VEGFR1 show excessive disorganized endothelium and are also nonviable (27). Interestingly, in addition to its well recognized role in angiogenesis, VEGF-A has also been shown in recent work to be directly neuroprotective in rodent models of neurodegeneration (28, 29); thus, its effects within the CNS are more complex than previously appreciated. In the inflamed CNS, VEGF-A and its regulatory transcription factor hypoxia-inducible factor-1 α are expressed by

reactive astrocytes (16, 20), and astrocytic end-feet lie in close proximity to microvascular endothelium in the brain and spinal cord (30). Astrocytes have been consistently linked to BBB induction during development and its disruption under inflammatory conditions (10, 15), and VEGF-A has been implicated as an inducer of BBB breakdown (19, 20), but its mechanism of action has remained unknown.

Although CLN-3, CLN-5, and CLN-12 are all expressed by BMVECs (4), compelling evidence implicates CLN-5 as primarily responsible for determining the high trans-endothelial resistance of BBB tight junctions (5, 6). Within the brain, CLN-5 is restricted to endothelium and expression of its mRNA within this compartment is more than 750 times that of CLN-12 (5). Transfection of CLN-5 into cell lines is associated with induction of barrier properties, whereas CLN-5^{-/-} mice show selective BBB opening and die perinatally (6). These data suggest CLN-5 as a key determinant of trans-endothelial resistance at the BBB, and its disruption has previously been linked to barrier breakdown in glioblastoma multiforme, a neoplastic disorder of human CNS (31). More recently, down-regulation of CLN-5, OCLN, and ZO-1 has also been shown to result in disruption of the blood-spinal cord barrier in SOD1 mutant models of amyotrophic lateral sclerosis (32). Interestingly, the mechanism underlying this latter effect involves direct toxicity of mutant SOD1 on endothelial cells as opposed to the VEGF-mediated down-regulation observed in our experiments.

The role of OCLN in determining the formation and properties of tight junctions appears more complex. Like claudins, OCLN is a component of tight junction strands (7), but strands also form in OCLN-deficient cells (8), and the complex phenotype of OCLN^{-/-} mice is not clearly related to tight junction abnormalities (9). However, phosphorylation of the cytoplasmic domain of OCLN correlates with tight junction formation (33) and has been shown to regulate junction permeability (34). Both external loops, as well as the transmembrane and the cytoplasmic domains of OCLN, are important for regulation of paracellular permeability (35), and studies have also shown that OCLN is responsible for sealing of tight junctions (36). Thus, available data suggest that the function of OCLN may be to regulate rather than establish barrier properties. Recently, two studies have reported changes in endothelial OCLN in the spinal cord in EAE. The first showed dephosphorylation of OCLN in EAE lesions (37) and the second demonstrated disruption of OCLN and ZO-1 (38). Our data extend these observations and suggest that loss of endothelial CLN-5 is a key event in inducing BBB breakdown, but they do not rule out a significant role for OCLN in the response. The BBB opening observed in CLN5^{-/-} mice is selective for small molecules (<800 D) (6), whereas the disruption in CNS inflammation is more severe and less size-selective. It is possible that that, whereas loss of CLN-5 is important for initiation of barrier disruption *in vivo*, loss of OCLN may exacerbate the phenotype. This interpretation is subject to testing but would be compatible with the known functions of both molecules.

The effects of VEGF-A on CLN-5 and OCLN in our experiments on BMVECs occurred at both the RNA and protein levels and appeared highly specific. VEGF-A had no effect on JAM-1, cingulin, CASK, or ZO-1. The mechanism underlying this specificity is not clear, and the recent characterization of the CLN-5 promoter may prove helpful in this context (39). Claudins are reorganized and recycled in cells as part of normal junction maintenance (40), and the striking alterations in CLN-5 and OCLN observed in our experiments may reflect this rapid turnover. However, as VEGF-A is a potent mitogen for BMVECs (27), it is also possible that its effects on CLN-5 and OCLN are part of a more long-lasting switch to a mitotic phenotype.

Recent reports indicate that therapies designed to restrict BBB disruption represent a potentially important area in research into inflammatory CNS disorders (2). To design effective therapeutic strategies, it is imperative to understand the mechanisms governing the BBB breakdown that is a prominent feature of these patholo-

gies, while taking into account other known functions of the molecules involved. Our results suggest that VEGF-A-induced down-regulation of CLN-5 constitutes an important mechanism in BBB disruption in the inflamed brain and spinal cord. These events may represent a potential target for therapeutic intervention.

Materials and Methods

Cytokines/Growth Factors. Human IL-1 β and FGF-1 and mouse VEGF₁₆₅ were from Peptidech; human IFN γ , TGF β 1, IL-6, and VEGF₁₆₅ from R&D Systems; and human VEGF-C from Biovision. Based on previous studies, human VEGF-A was routinely used at 100 ng/mL, other factors 10 ng/mL (16). Mouse VEGF₁₆₅ was used at 20 ng/ μ L. Flt-1/Fc (R&D Systems) was used at 40 ng/mL (24).

Cell Culture. Primary human fetal astrocyte cultures were established from 3 different brains, as described (16). Primary human or bovine BMVEC were purchased from Cell Systems Inc. and cultured in complete serum containing (CSC) medium. All studies were approved by the appropriate Institutional Review Board.

Expression Constructs. Human CLN-5 in pENTR221 (Invitrogen) was transferred to pcDNA-DEST40 (Invitrogen) under CMV (pDCLN5). Vector control was pcDNA-DEST40 (pDEST). Human OCLN in pCMV-SPORT6 was from ATCC (pSO-CLN). Vector control was pCMV-SPORT6 (pS6). Expression of recombinant CLN-5 and OCLN, and lack of sensitivity to VEGF-A were confirmed by nucleofection into negative cell lines (CLN-5 - HEK; OCLN - Hs578T)²⁵, or BMVEC.

Permeability Assays. BMVEC were plated onto 0.4- μ m pore culture inserts (Corning) and left to reach confluence for 10–14 d. Cultures were then treated

as specified and at times shown dextran-FITC (100 μ g/mL, 40 or 3 Kd, Molecular Probes) in growth factor- and serum-free CSC medium 0.1% BSA was added to the upper chamber and its accumulation in the lower chamber measured over 30 min to 4 hr (23).

Immunohistochemistry. Animals were perfused with 4% paraformaldehyde at times specified. Embedding and immunostaining were performed as published (16), except where noted. For claudins, prior to blocking, sections were soaked in EDTA, pH 8, 100°C. For OCLN, sections were treated with 0.5 mg/mL protease XIV (Sigma-Aldrich) at 37°C for 5 min. Primary antibodies were used at 1:100, except CLN-5 (1:50), fibrinogen (1:1,000), and albumin (1:1,000). Samples were examined as above and Z-series stacks collected with z = 1 μ m.

Statistical Analyses. For multiple comparisons, 1-way ANOVA followed by Bonferroni post test was used. Student's t test was used to compare 2 groups of matched samples. The Spearman rank correlation coefficient was used to test for correlation of 2 variables. In all cases, $P < 0.05$ was considered significant. For further details, please see *SI Materials and Methods*.

ACKNOWLEDGMENTS. The authors thank Dr. Bradford Poulos, Director of the HFTR at Albert Einstein College of Medicine, for tissue collection, and the Mount Sinai School of Medicine (MSSM) Shared Resource Facility. We thank Beth Zvilovitz for help with paracellular permeability assays, and Dr. Carmen Melendez-Vasquez, Prof. Celia Brosnan, and Prof. Cedric Raine for input on the manuscript. This work was supported by United States Public Health Service Grants NS46620 and NS056074 (to G.R.J.), National Multiple Sclerosis Society Grants FG1739 (to Y.Z.) and RG3874 (G.R.J.), and by the Jayne and Harvey Beker Foundation (G.R.J.). The MSSM Microscopy Shared Resource Facility is supported in part by funding from National Institutes of Health/National Cancer Institute Grant R24 CA095823.

- Zlokovic BV (2008) The blood-brain barrier in health and chronic neurodegenerative disorders. *Neuron* 57:178–201.
- Abbott NJ, Rönnbäck L, Hansson E (2006) Astrocyte-endothelial interactions at the blood-brain barrier. *Nat Rev Neurosci* 7:41–53.
- Tsukita S, Furuse M (2002) Claudin-based barrier in simple and stratified cellular sheets. *Curr Opin Cell Biol* 14:531–536.
- Morita K, Sasaki H, Furuse M, Tsukita S (1999) Endothelial claudin: claudin-5/TM6CF constitutes tight junction strands in endothelial cells. *J Cell Biol* 147:185–194.
- Ohtsuki S, et al. (2007) Exogenous expression of claudin-5 induces barrier properties in cultured rat brain capillary endothelial cells. *J Cell Physiol* 210:81–86.
- Nitta T, et al. (2003) Size-selective loosening of the blood-brain barrier in claudin-5-deficient mice. *J Cell Biol* 161:653–660.
- Furuse M, et al. (1993) Occludin: a novel integral membrane protein localizing at tight junctions. *J Cell Biol* 123:1777–1788.
- Saitou M, et al. (1998) Occludin-deficient embryonic stem cells can differentiate into polarized epithelial cells bearing tight junctions. *J Cell Biol* 141:397–408.
- Saitou M, et al. (2000) Complex phenotype of mice lacking occludin, a component of tight junction strands. *Mol Biol Cell* 11:4131–4142.
- Janzer RC, Raff MC (1987) Astrocytes induce blood-brain barrier properties in endothelial cells. *Nature* 325:253–257.
- Lindahl P, Johansson BR, Leveén P, Betsholtz C (1997) Pericyte loss and microaneurysm formation in PDGF-B-deficient mice. *Science* 277:242–245.
- Tallquist MD, French WJ, Soriano P (2003) Additive effects of PDGF receptor beta signaling pathways in vascular smooth muscle cell development. *PLoS Biol* 1:E52.
- Bunge RP, Bunge MB, Ris H (1960) Electron microscopic study of demyelination in an experimentally induced lesion in adult cat spinal cord. *J Biophys Biochem Cytol* 7:685–696.
- Schachtrup C, et al. (2007) Fibrinogen inhibits neurite outgrowth via beta 3 integrin-mediated phosphorylation of the EGF receptor. *Proc Natl Acad Sci USA* 104:11814–11819.
- Bush TG, et al. (1999) Leukocyte infiltration, neuronal degeneration, and neurite outgrowth after ablation of scar-forming, reactive astrocytes in adult transgenic mice. *Neuron* 23:297–308.
- Argaw AT, et al. (2006) Interleukin-1 β induces blood-brain barrier permeability via reactivation of the hypoxia-angiogenesis program. *J Immunol* 177:5574–5584.
- Carmeliet P, et al. (1996) Abnormal blood vessel development and lethality in embryos lacking a single VEGF allele. *Nature* 380:435–439.
- Ferrara N, et al. (1996) Heterozygous embryonic lethality induced by targeted inactivation of the VEGF gene. *Nature* 380:439–442.
- Dobrogowska DH, Lossinsky AS, Tarnawski M, Vorbrodt AW (1998) Increased blood-brain barrier permeability and endothelial abnormalities induced by vascular endothelial growth factor. *J Neurocytol* 27:163–173.
- Proescholdt MA, Jacobson S, Tresser N, Oldfield EH, Merrill MJ (2002) Vascular endothelial growth factor is expressed in multiple sclerosis plaques and can induce inflammatory lesions in experimental allergic encephalomyelitis rats. *J Neuropathol Exp Neurol* 61:914–925.
- Chen L, Brosnan CF (2006) Exacerbation of experimental autoimmune encephalomyelitis in P2X7R^{-/-} mice: evidence for loss of apoptotic activity in lymphocytes. *J Immunol* 176:3115–3126.
- Kristensson K, Wiśniewski HM (1977) Chronic relapsing experimental allergic encephalomyelitis. Studies in vascular permeability changes. *Acta Neuropathol* 39:189–194.
- Song L, Ge S, Pachter JS (2007) Caveolin-1 regulates expression of junction-associated proteins in brain microvascular endothelial cells. *Blood* 109:1515–1523.
- Conn G, et al. (1990) Amino acid and cDNA sequences of a vascular endothelial cell mitogen that is homologous to platelet-derived growth factor. *Proc Natl Acad Sci USA* 87:2628–2632.
- Polette M, et al. (2005) Membrane-type 1 matrix metalloproteinase expression is regulated by zonula occludens-1 in human breast cancer cells. *Cancer Res* 65:7691–7698.
- Shalaby F, et al. (1995) Failure of blood-island formation and vasculogenesis in Flk-1-deficient mice. *Nature* 376:62–66.
- Fong GH, Rossant J, Gertsstein M, Breitman ML (1995) Role of the Flt-1 receptor tyrosine kinase in regulating the assembly of vascular endothelium. *Nature* 376:66–70.
- Jin KL, Mao XO, Greenberg DA (2000) Vascular endothelial growth factor: direct neuroprotective effect in *in vitro* ischemia. *Proc Natl Acad Sci USA* 97:10242–10247.
- Storkebaum E, et al. (2005) Treatment of motoneuron degeneration by intracerebroventricular delivery of VEGF in a rat model of ALS. *Nat Neurosci* 8:85–92.
- Reichenbach A, Wolburg H (2004) Astrocytes and ependymal glia. *Neuroglia*, eds Kettemann H, Ransom BR (Oxford Univ. Press, New York), 2nd Ed, pp 19–35.
- Liebner S, et al. (2000) Claudin-1 and claudin-5 expression and tight junction morphology are altered in blood vessels of human glioblastoma multiforme. *Acta Neuropathol* 100:323–331.
- Zhong Z, et al. (2008) ALS-causing SOD1 mutants generate vascular changes prior to motor neuron degeneration. *Nat Neurosci* 11:420–422.
- Sakakibara A, Furuse M, Saitou M, Ando-Akatsuka Y, Tsukita S (1997) Possible involvement of phosphorylation of occludin in tight junction formation. *J Cell Biol* 137:1393–1401.
- Hirase T, et al. (2001) Regulation of tight junction permeability and occludin phosphorylation by RhoA-p160ROCK-dependent and -independent mechanisms. *J Biol Chem* 276:10423–10431.
- Balda MS, Flores-Maldonado C, Cerejido M, Matter K (2000) Multiple domains of occludin are involved in the regulation of paracellular permeability. *J Cell Biochem* 78:85–96.
- Lacaz-Vieira F, Jaeger MM, Farshori P, Kachar B. Small synthetic peptides homologous to segments of the first external loop of occludin impair tight junction resealing. *J Membr Biol* 168:289–297.
- Morgan L, et al. (2007) Inflammation and dephosphorylation of the tight junction protein occludin in an experimental model of multiple sclerosis. *Neuroscience* 147:664–673.
- Kebir, et al. (2007) Human TH17 lymphocytes promote blood-brain barrier disruption and central nervous system inflammation. *Nat Med* 13:1173–1175.
- Burek M, Förster CY (2008) Cloning and characterization of the murine claudin-5 promoter. *Mol Cell Endocrinol*, in press.
- Matsuda M, Kubo A, Furuse M, Tsukita S (2004) A peculiar internalization of claudins, tight junction-specific adhesion molecules, during the intercellular movement of epithelial cells. *J Cell Sci* 117:1247–1257.